Wuhan University
Journal of Natural Sciences

2010, Vol.15 No.2, 176-184

Article ID 1007-1202(2010)02-0176-09
DOI 10.1007/s11859-010-0217-6

Microstructure and Element Composition of Shell Plates of *Liolophura japonica*

□ **CHEN Daohai**[1,2]

1. College of Fisheries, Ocean University of China, Qingdao 266003, Shangdong, China;

2. Life Science and Technology School, Zhanjiang Normal University, Zhanjiang 524048, Guangdong, China

© Wuhan University and Springer-Verlag Berlin Heidelberg 2010

Abstract: The microstructure characteristics of shell plates of chiton *Liolophura japonica* Lischke were analyzed using environmental scanning electron microscopy (ESEM). The results show that the internal structure of the shell plate of chiton *Liolophura japonica* is composed of seven calcium layers which were crossed lamellar crystallites, homogeneous structure, granular crystallites, and trabecular type crystallites. The element compositions of shell plates were analyzed using X-ray photoelectron spectroscopy (XPS). The results determined by XPS show that the surface chemical states of various layers are different. There are 13 elements (Na, O, N, C, S, P, Ca, Cl, Si, Al, K, Fe, Mg) on the shell plate of chiton *L. japonica*. Among the 13 elements, 11 are on the outside pigment layer except K and S. Among seven layers of shell plate, there is the largest quantity of elements on the outside pigment layer, and the least quantity of elements is on layer C (Articulamentum auctorum). There are 7 elements on the layer C (Articulamentum auctorum). Besides calcium carbonate, there are some inorganic compounds on the shell plate, such as NaCl, MgO, Al_2O_3, silicate, sulfate and phosphate. There are some organic chemical components, such as carbohydrate, organic sulfide, and organic nitride on the shell plates.

Key words: *Liolophura japonica*; environmental scanning electron microscope; X-ray photoelectron spectroscopy (XPS); microstructure of shell plate

CLC number: Q 959

Received date: 2009-05-16

Foundation item: Supported by the Foundation of National 908 Program (908-01-ST12) and the National High Technology Research and Development Program of China(863 Program) (2007AA09Z433)

Biography: CHEN Daohai (1963-), male, Professor, Ph. D., research direction: structural biology. E-mail:dhchen11@21cn.com

0 Introduction

In 1930, for the first time, Boggild made a relatively comprehensive research on the interior structure of the mollusk shell according to its mineralogy and crystallographic characteristics; many data about microcrystal structures of shells including that from monoplacophora, bivalve, gastropod and cephalopod have been reported[1-10]. A lot of researchers thought that the most typical microstructure of the shell of mollusks is made of aragonite crossed lamellar[2,9]. Someone considered that there are nine kinds of microcystal structures of the shell of mollusks: simple prismatic, spherulitic prismatic, columnar nacre, sheet nacre, comarginal crossed lamellar, sagittal developed crossed lamellar, irregular complex crossed lamellar, intersected crossed platy and homogeneous[11]. In contrast, among polyplacophora animals, only one article about the interior structures of the shell plate of *Chiton olivaceus* had been reported[12]. Laghi described the layered shell plate structure of *Chiton olivaceus* in his paper. However, the paper did not illustrate the crystallographic characteristics of *Chiton olivaceus*, nor was the chemical composition of interior structures of the shell plate analyzed.

XPS or X-ray photoelectron spectroscopy, is a new surface analysis method that evaluates conveniently the chemical binding state of the solid sample. It is possible to realize the depth analysis of a sample in XPS analysis method[13]. *Liolophura japonica* is a large sized chiton that is distributed widely in

the coastal regions of China Sea. It has very wide and thick shell plates that can provide us the means to study the interior microstructures, and is an ideal material to analyse chemical composition on shell plates.

The surface and internal microcystal structures of the shell plate based on *L. japonica* are reported. Also, the surface of the substances composition of all layers of the shell plate were analysed by XPS in this paper. It provides the basic data for exploring the shell plate's biomineralization mechanism and formation process. Researching its structure and peculiar formation process may provide reference in manufacturing efficient, energy saving and environmentally friendly materials[14,15].

1 Materials and Methods

1.1 Materials and Instruments

Chiton samples were taken from Naozhou Island, Zhanjiang (20°56′N, 110°36′E).

Environmental scanning electron microscope (ESEM), (Model: Amray 1910F); Scanning electron microscope (SEM) (Model: PHILIPS XL-EDAX, Holand); ion sputtering equipment (Model: E-1010, HITACHI, Japan); Critical drying device (Model: HCP-Z, HITACHI, Japan); X-ray photoelectron spectroscopy (XPS) (Model: AXIS Ultra, British Kratos Co.).

1.2 Methods

The shell plates are taken off from the back of chiton, rinsed with tap water, immersed in 25% (W∶V) sodium hypochlorite for 2 h to remove impurities on the surface of the shell plate, and its structure with dissection light microscope and ESEM were observed. Treatment of ESEM sample follows the routine method.

Several small segments from the shell plates were taken at different locations, with mechanical separation. Epoxy resin was embedded along every section and polished; they can be used for XPS analysis. To expose microstructures, the sample was polished and fractured with acids and enzymes then the shell was observed a with scanning electron microscope.

Fixative and etching solutions such as a mixture of acetic acid 1%(V∶V)+ glutaraldehyde 12%(W∶V) were used to preserve the organic matrices. These matrices were partially destroyed by enzymes at 38 ℃ (1 mg/mL protease in Hepes pH 7.8, 1 mg/mL trypsine in Hepes pH 7.8 (offered by Sigma Co), to reveal the detailed shape of the microstructure. The purpose of using pH7.8 is to minimize the dissolution of carbonate of the shell.

Test conditions and method: use Al target X-ray source with homochromic gauge (Al$K\alpha$, $h\nu$=1 486.71 eV), power 225 W (operation voltage 15 kV, emission current 15 mA). Polluted carbon (inner target) 234.8 eV; min. energy definition 0.48 eV, min. XPS analysis area 15 μm; Vision (PR2.1.3) and Casa XPS software (2.3.12 Dev 7) for data processing.

2 Results

2.1 Microstructure of Shell Plate of *L. japonica*

The thickness and microstructure of shell plates of *L. japonica* are different at different positions. In ESEM, it is observed clearly that the cross-section of chiton shell plate is comprised of seven layers (Fig. 1): layer A, layer B, layer C (Fig.1: A), layer D, Layer E, layer F, and layer G.. Sutural plates or insertion plates appear symmetrically at both sides of the shell plate. The slits are extended from the edge of insertion plates (Fig.1: B). The thickness at the intermediate position of the shell plate is 1.5 mm (n=20). Many tiny granules with pore canals extrude on the surface of head valve (Fig.1: C).

① Layer A: the out pigment layer, called "tegmentum auctorum", consists of granular crystallites (Fig.1: M). This layer shows a homogeneous crystal structure in the outer side and a trabecular crystal structure in the inner side. The middle of the valve (jugum), jugal joists having a trabecular crystal structure, is located. Homogeneous tegmentum encloses the joists evenly. Girdle covered with calcareous spinules, which are comprised of granular crystallites (Fig.1: O).

② Layer B: called "mesostracum", consists of two sublayers both with crossed lamellar structure, a row of pores separates the sublayers. Pore canals (Fig.1: A, E) are 50-140 μm in diameter

③ Layer C: called "Articulamentum auctorum", Sutural plate and insertion plate arranged symmetrically at both sides. The thickest location on layer C is about 600 μm (Fig.1: A, F), the structure of articulamentum is trabecular crystal type; the pattern is more obvious and regular at the tooth constituting the insertion plate.

④ Layer D: crossed lamellar, the layer combines with the layer B along the edge of pleural area jugum the posterior edge of the lateral area. Layer B+D are flat, and also called "Myostracum", consisting of crossed lamellae crystallites; adjacent lamellae shows a right angle (Fig.1: H, K).

⑤ Layer E: the calcareous substance appearing symmetrically at the impression of lateropedal. The thickest on layer E is about 400 μm (Fig.1: A, D), con-

sisting of trabecular crystallites, laying irregularly.

⑥ Layer F: called the "Hypostracum auctorum", is very prominent and has an open V-shape on the ventral surface of shell plates; this layer is very thick in the center area, consisting of sagittal developed lamellae and granule layer; between lamellae is a granule layer (Fig.1: G, I, L). Each lamellar is formed by regular and parallel arrangement of tiny elongate crystallites (third-order lamellae of thickness 0.3 μm). The relationships between the three order structures are as follows: third-order

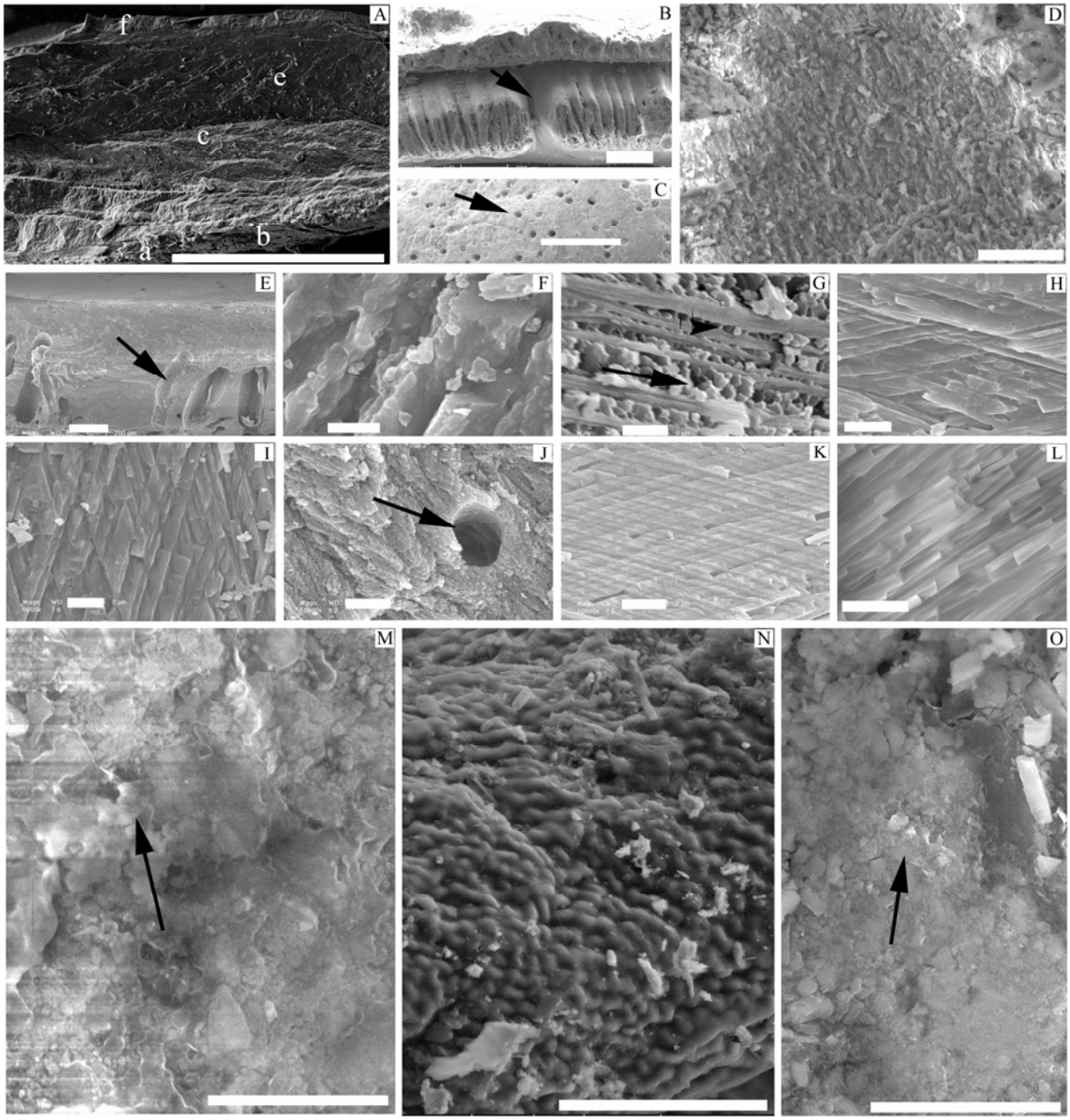

Fig. 1 Microstructure of shell plates of *Liolophura japonica*

A: intermediate valve of *Liolophura japonica*, a-f: showing layer a to layer f, Bar =1 mm; B: in front of intermediate valve of *Liolophura japonica*, the arrow showing slits; C: head valve of *Liolophura japonica*, the arrow showing granules on shell surface. Bar =100 μm; D: intermediate valve of *Liolophura japonica*, showing layer E, Bar=20 μm; E: intermediate valve of *Liolophura japonica*, the arrow showing pore, Bar=200 μm; F: intermediate valve of *Liolophura japonica*, Showing trabecular structure of layer C, Bar =2 μm; G: intermediate valve of *Liolophura japonica*, sagittal section of layer F, aragonitic crystallites organized into first order lamellae are visible, of which the thickness of lamellae is about 3 μ, the arrow showing granular crystallites filling with between aragonitic crystallites, Bar =2 μm; H: intermediate valve of *Liolophura japonica*, transversal section crossed-lamellar structure of layer D is visible on the contact plane between two adjacent first order lamellae, the angle between crystallites (3rd order lamellae) is about 90, Bar =2 μm; I: intermediate valve of *Liolophura japonica*, sagittal section crossed lamellar structure of layer D, Bar =2 μm; J: intermediate valve of *Liolophura japonica*, crossed-lamellar, the arrow showing pore, Bar=2 μm; K: intermediate valve of *Liolophura japonica*, crossed lamellar structure of layer F, Bar=2 μm; L: intermediate valve of *Liolophura japonica*, sagittal section crossed lamellar structure of layer F, Bar =2 μm; M: intermediate valve of *Liolophura japonica*, the arrow showing surface granules structure of layer A, Bar =2 μm; N: intermediate valve of *Liolophura japonica*, showing shell ventral surface, Bar =50 μm; O: intermediate valve of *Liolophura japonica*, the arrow showing surface granules structure of layer A corresponding to spicule. Bar =5 μm

nanocrystals lamellae constitutes second-order lamellae, and second-order lamellae arranges in turn and forms a large unit, called first-order lamellae (about 3 μm thick)

⑦ Layer G: the calcareous substance appeared symmetrically at transverse muscle.

Layer E and layer G have homogeneous structure. Sutural plate surface enamel is shown in (Fig.1: N).

2.2 Combined Form of Elements in the Shell Plates' Back Surface of *L.japonica*

Examining the elements of the shell plates' back surface of *L. japonica* with XPS at the depth of 3-5 nm, 11 elements are found (Fig.2). The atomic percentage of the elements (mol) are as follows: Na 0.88%, Fe 0.61%, O 28.82%, N 3.68%, C 56.19%, P 0.45%, Ca 1.3%, Cl 0.45%, Si 4.71%, Al 2.47%, Mg 0.46%. The combined forms of these elements are shown in the following spectrum (Fig. 2).

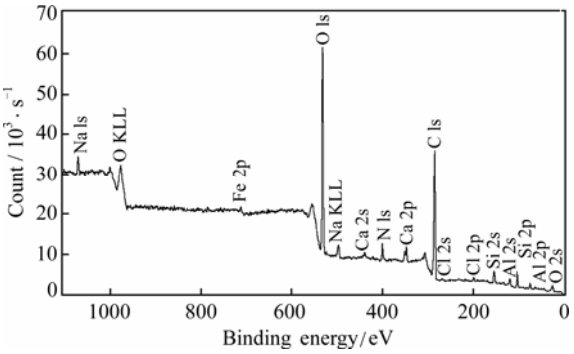

Fig. 2 X-ray photoelectron spectroscopy image on the dorsal surface of shell inner structure of *L.japonica*

2.2.1 Forms of Si on the back surface of shell plates of *L. japonica*

Peak of electronic binding energy of Si on the shell plates' back surface of *L. japonica* is 102.56 eV, indicating the element exists in the form of pure silicate (Fig.3).

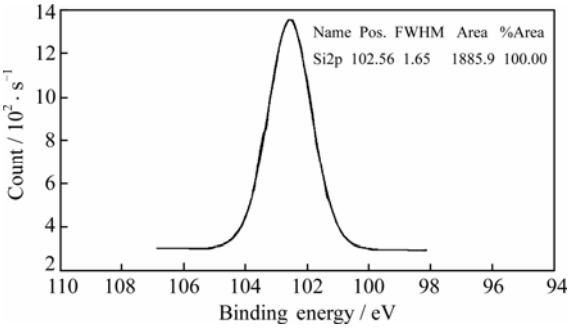

Fig. 3 X-ray photoelectron spectroscopy image of Si element on the dorsal shell surface of *L. japonica*

Pos: Position; FWHM: full width at half maximum; Area: peak area; % Area: Peak area percentage

2.2.2 Forms of Al on the back surface of shell plates of *L. japonica*

Peak of electronic binding energy of Al on the shell plates' back surface of *L. japonica* is 74.3 eV, it is shows that there is only one form of oxide existing: Al_2O_3 (Fig.4).

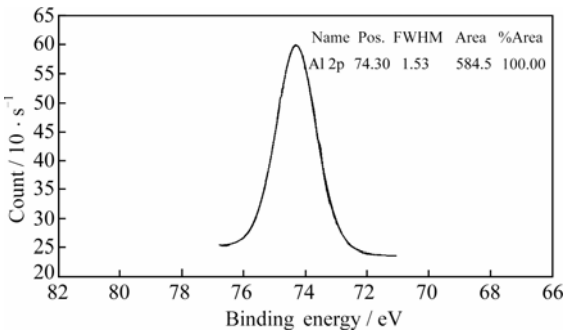

Fig. 4 X-ray photoelectron spectroscopy image of Al element on the dorsal shell surface of *L. japonica*

Pos: Position; FWHM: full width at half maximum; Area: peak area; % Area: Peak area percentage

2.2.3 Forms of C element on the back surface of shell plates of *L. japonica*

Spectrum chart and peak fit chart of C 1s on back surface of shell plates of *L. japonica*. Judging from Fig.5, C 1s spectrum fits the division of peaks through curves, which denotes that C exists in four forms in surface structure. The 284.8 eV peak belongs to the aromatic unit and its replacement alkyl (C—H), and denotes that there are hydrocarbons on the shell surface. The 286.28 eV peak belongs to hydroxybenzene carbon or aether carbon (C—O), which denotes that cellulose and semi-cellulose exist on the surface of the shell. The 287.86 eV peak belongs to carbonyl (C═O), which denotes that it contains mainly aldehyde, ketone and acetal. The 289.22 eV peak belongs to carboxyl or ester (COO—), which denotes that organic acids exist in the shell.

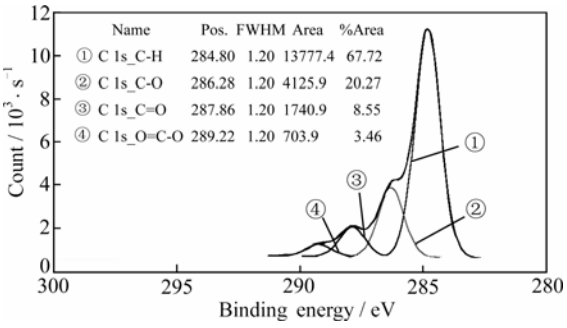

Fig. 5 X-ray photoelectron spectroscopy image of C element on the dorsal shell surface of *L. japonica*

Pos: Position; FWHM: full width at half maximum; Area: peak area; % Area: Peak area percentage

According to its binding energy site, the element existing in the form of C belongs to C—H, C—O, C═O and O═C—O, respectively, the content is counted from corresponding peak area, C—H 38.05%, C—O 11.39%, C═O 4.8%, O═C—O: 1.94%.

2.2.4 Forms of Ca on the back surface of shell plates of *L. japonica*

Spectrum chart of Ca on the back surface of shell plates indicates (Fig.6): Ca on the back surface of *L. japonica* has two spectrum peaks, the binding energy peak of Ca in 2p electron of lamella is 347.25 eV, shown in Ca 2p 3/2, it exists in the form of CaO or $CaCO_3$; Another peak of the electronic binding energy of atom Ca in 2p lamella is 350.81 eV, shown in Ca 2p 1/2. The percentage of the two forms are 2p 3/2 (CaO or $CaCO_3$) 66.69% and 2p 1/2 33.31%.

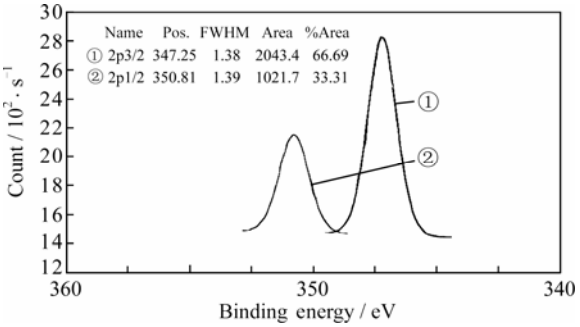

Fig. 6 X-ray photoelectron spectroscopy image of Ca element on the dorsal shell surface of *L. japonica*

Pos: Position; FWHM: full width at half maximum; Area: peak area; % Area: Peak area percentage

2.2.5 Forms of Cl on the back surface of shell plates of *L. japonica*

PE Spectrum chart of Cl on back shell plates' surface of *L. japonica* indicates (Fig.7): element Cl on lamella periostracum has two spectrum peaks, electronic binding energy peak of Cl atom 2p 3/2 is 197.98 eV, exists in the form of NaCl; Cl 2p 1/2 peak value is 199.58 eV. The percentage of the two forms are 2p 3/2 (NaCl) 66.68% and 2p 1/2 33.32%.

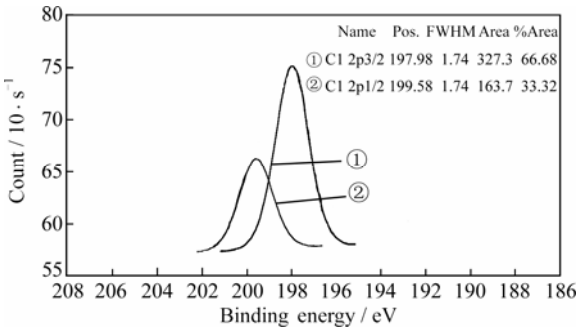

Fig. 7 X-ray photoelectron spectroscopy image of Cl element on the dorsal shell surface of *L. japonica*

Pos: Position; FWHM: full width at half maximum; Area: peak area; % Area: Peak area percentage

2.2.6 Combined form of Fe on the back surface of shell plates of *L. japonica*

Electronic photoelectric energy peak of Fe on the back shell plate's surface of *L. japonica* is 712.01 eV, only one form of Fe^{2+} (Fig.8). To analyze according to its regional distributed element combination, Fe element exists likely in the form of $FeCl_2$.

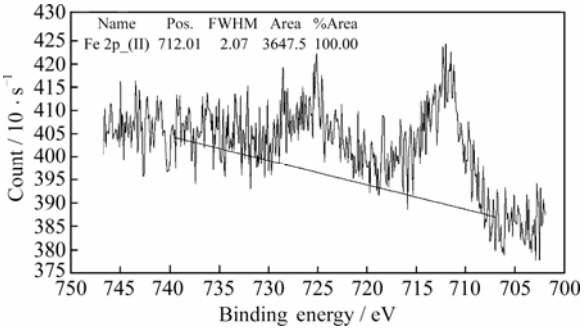

Fig. 8 X-ray photoelectron spectroscopy image of Na element on the dorsal shell surface of *L. japonica*

Pos: Position; FWHM: full width at half maximum; Area: peak area; % Area: Peak area percentage

2.2.7 Forms of Mg on the back surface of shell plates of *L. japonica*

The peak of electronic binding energy of Mg on the back surface of shell plates of *L. japonica* is 49.94 eV; it is proven to exist in only one form: Mg^{2+} (Fig.9). Its combined form is MgO.

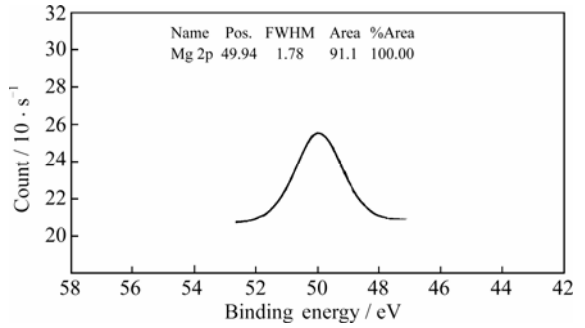

Fig. 9 X-ray photoelectron spectroscopy image of Mg element on the dorsal shell surface of *L. japonica*

Pos: Position; FWHM: full width at half maximum; Area: peak area; % Area: Peak area percentage

2.2.8 Combined form of N element on the back surface of shell plates of *L. japonica*

PE Spectrum Chart of element N on shell plate back surface indicates (Fig.10): the N element on shell plates back surface of *L. japonica* has two spectrum peaks, electron binding energy peak of atom N 1s in lamella is 399.88 eV, shown in N 1s _a, N1s-a exists in the form of HN—C═O; Another peak of electron binding energy of

atom N in 1s lamella is 401.97 eV, shown in N 1s_b, exists in the form of N1s-b C—NH_2, C—NH^{3+}.

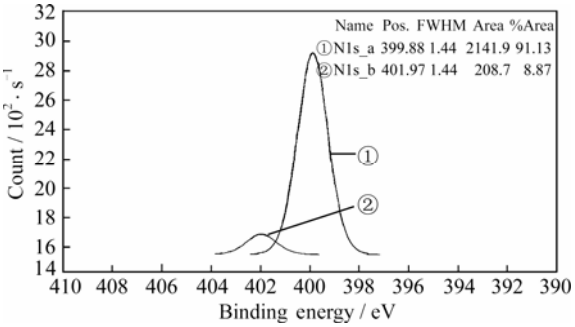

Fig. 10 X-ray photoelectron spectroscopy image of N element on the dorsal shell surface of *L. japonica*

Pos: Position; FWHM: full width at half maximum; Area: peak area; % Area: Peak area percentage

2.2.9 Combined form of element Na on the back surface of shell plates of *L. japonica*

Electronic photoelectric energy peak of element Na on shell plate back surface of *L. japonica* is 1 071. 41 eV, in only one form: Na^+ (Fig.11), analyzed according to its regional distributed element combination, element Na exists likely in the form of NaCl.

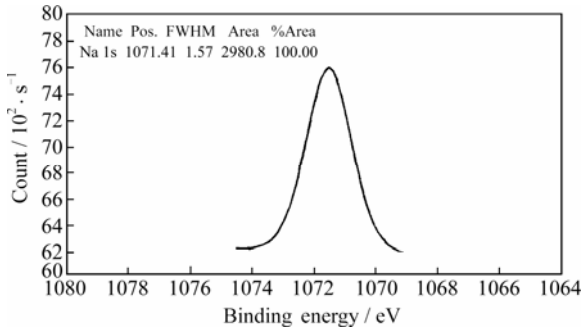

Fig. 11 X-ray photoelectron spectroscopy image of Na element on the dorsal shell surface of *L. japonica*

Pos: Position; FWHM: full width at half maximum; Area: peak area; % Area: Peak area percentage

2.2.10 Combined form of O element on the back surface of shell plates of *L. japonica*

O 1s XPS spectrum and test data of shell plates back surface refers to Fig.12, O1s spectrum is comprised of two peaks: peak of O 1s_a electronic binding energy is 531.47 eV, peak of O 1s_b electronic binding energy is 532.54 eV, which represents the linkage mode between O and C. C—O with higher binding energy indicates that O bonds with C through the single linkage, shown in O 1s_a. The C═O with lower binding energy indicates that O bonds with C through double bond linkage, shown in O 1s_b. O 1s_a content is 18.49%, O 1s_b content is 10.33%. It showed that the binding mode between O and C on the surface is mainly single linkage, whereas the binding through double bond is relatively rare.

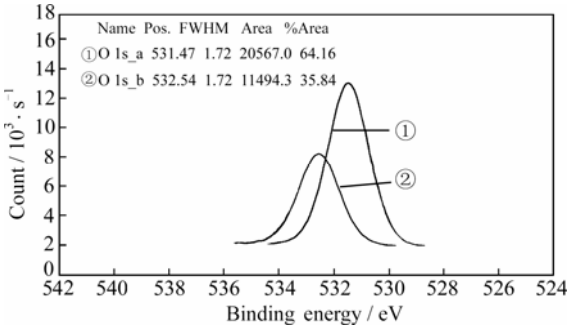

Fig. 12 X-ray photoelectron spectroscopy image of O element on the dorsal shell surface of *L. japonica*

Pos: Position; FWHM: full width at half maximum; Area: peak area; % Area: Peak area percentage

2.2.11 Forms of P on the back surface of shell plates of *L. japonica*

PE Spectrum Chart of element P on the back surface of shell plates indicates (Fig.13): the element P on the shell plates back surface of *L. japonica* has two spectrum peaks, 2p 3/2 electron of lamella, its binding energy peak is 133.03 eV, which exists in the form of P_2O_5 or phosphate, 2p 1/2 electron of lamella, its binding energy peak is 133.87 eV. The percentage of the two forms are 2p 3/2 66.67% and 2p 1/2-33.33%.

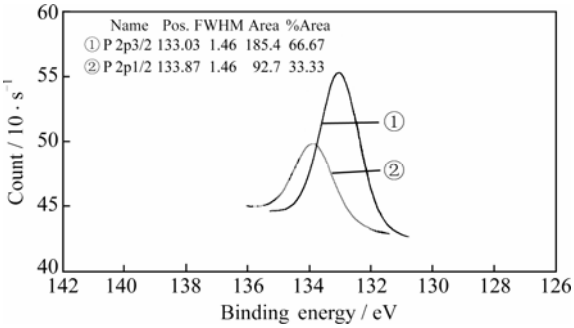

Fig. 13 X-ray photoelectron spectroscopy image of P element on the dorsal shell surface of *L. japonica*

Pos: Position; FWHM: full width at half maximum; Area: peak area; % Area: Peak area percentage

2.3 Comparison on Contents of Elements among the Shell Layers of *L. japonica*

XPS test results reveal that all layers of shell plates contain seven elements Na, O, N, C, P, Ca, Si. The elements on layer C of shell plates of *L. japonica* are relatively few, excluding S, Cl, Al, K, Fe and Mg. However, those 6 elements were detected in other samples. The elements in the surface of periostracum are the most abundant. Among 13 detected elements, except for S and K, other 11 elements exist in the periostracum surface layer. Element contents of all layers are shown in Table 1.

Table 1 Comparison on contents of elements among the shell layers of *L. japonica* %

Layers	Na	O	N	C	S	P	Ca	Cl	Si	Al	K	Fe	Mg
Dorsal surface	0.88	28.82	3.68	56.19	—	0.45	1.3	0.45	4.71	2.47	—	0.61	0.46
Layer A	0.59	35.73	5.03	48.38	0.69	0.74	6.7	0.12	1.24	0.46	0.31	—	—
Layer C	0.24	21.07	6.53	70.27	—	1.00	0.67	—	0.21	—	—	—	—
Layer B	0.18	20.16	10.09	67.82	0.41	0.33	0.69	0.16	0.15	—	—	—	—
Layer D	0.17	17.51	7.78	71.93	0.35	0.74	1.00	0.1	0.11	—	—	—	0.32
Layer E+G	1.99	26.81	2.31	59.88	0.28	0.56	5.25	2.43	0.49	—	—	—	—
Layer F	0.34	21.57	5.61	67.59	0.40	0.54	1.78	0.13	1.16	0.44	—	—	0.44
Ventral surface	0.60	22.37	7.86	64.99	0.22	0.81	2.58	0.37	0.03	—	—	—	0.17

2.4 Analysis for Matter of All Layers on the Shell Plates of *L. japonica*

According to elements detected in the samples and their binding energy peaks, all layers of the same organisms are detected to contain HN—C==O, C—NH_3^+, cellulose, aldehydes, ketones, acetal and organic acids. However, there is a certain difference in the inorganic composition. All layers contain NaCl, $CaCO_3$ and silicate. $FeCl_2$ had been detected only in the tegmentum auctorum. Except for tegmentum auctorum and layer C, the remaining layers were detected to contain sulphates. Al_2O_3 was detected in the pigment layer, layer A and layer F. MgO was detected in the tegmentum auctorum, layer D, layer F and the ventral surface of the shell plate. K, which was detected in layer A, may come from seawater environment.

As shown in Table 1, Mg is found on the ventral surface of the shell, layer D and F of the shell, in which lamella nanocrystal structure exists. Therefore, the presence of Mg is likely to relate to the lamella nanocrystal structure. We found that element Mg and S simultaneous existed on the ventral surface, layer D, layer E, layer F, and layer G. However, layer A only contains Mg without S. According to the binding energy peak of Mg, we would consider that the combined form of Mg in layer A is MgO; the combined form of S in layer E and layer G is organic sulfide (S-C); the combined form of S on the ventral surface of the shell plate, layer D and layer F, exists likely in the form of $MgSO_4$. The research reveals that besides the few K atoms on the surface of periostracum, no element K is found in other layers of the shell plate, which indicates K does not take part in the formation of nanocrystals. Fe on the shell plates surface of periostracum is in the form of Fe^{2+}.

3 Discussion

The results at present show that the nacre is not necessarily of an aragonite structure, for example, the hard section in the inner, medium and surface layer of the oyster shell are all of a calcite structure, and the loose section consists of calcite and calcite-Ⅱ structure. The black and lucent layer in the shell of *Pinna atropurpurea* is also of a calcite structure. Also, the prismatic is not necessarily of a calcite structure, e.g., the prismatic of the shell of *Cristaria plicata*, *Hyriopsis Cumingii*, *Anodonta woodiana*, *Macoma yoldiformis* or *Pinctada martensii* is comprised of aragonite. Also, periostracum is not comprised of only concholin, e.g., the periostracum of the shell plate of *Cristaria plicata*, *Hyriopsis Cumingii*, *Anodonta woodiana* or *Macoma yoldiformis* is comprised of aragonite. The periostracum of the shell plate of *Pinctada martensii* or *Pinna atropurpurea* is comprised of calcite[7,8].

Conus betulin and *Strombus lentiginosu* are all comprised of single aragonite[11]. The microstructures of the shell of *Neptunea cuming* are different in different positions[11]. The embryo shell and spiral have multilayer structure, the body spiral shell is a three-layer structure; at the edge of the shell mouth, there is a layer of columnar calcite. The degrees of arrangement order of aragonite crystal in *Neptunea cuming* shell increase from embryo shell, spiral to body spiral layer. Morphologically, the structure of gastropod is more complex and different than that of bivalve. Gastropod seashell presents mostly crossed lamellar; some possess prismatic structure[13].

The same as *Chiton olivaceus*[12], the interior structure of the shell plate of *L. japonica* also can be divided into 6 layers. The shell plate surface features on globular aggregates of calcite nanocrystallites are similar to that of the shell of *Austromegabalanus psittacus*[16]. Crossed lamellae exists not only in bivalve and in gastropod widely[17-19], but also in all chiton (Polyplacophoran) observed. The main composition of the shell plate of *L. japonica* is calcite all in columnar and parallel arrange-

ment, with many granules filled among them; the structure may be seen in the shell of *Austromegabalanus psittacus*[16]. When we observed the shell plate of *L. japonica*, the homogeneous crystal structure was found on layer A, layer E and layer G, but trabecular crystal structure in layer C. Multilevel ultrastructure of *L. japonica* is similar to the multilevel structure model put forward by Duaphin *et al*[18]. It shows that the internal structure of the shell plate of chiton is significantly different from mollusks such as gastropoda and bivalve.

Detected results from XPS, besides $CaCO_3$ and organic matter in the chiton shell plates, there are a lot of inorganic and organic composition of ingredients, which may play an important role in biomineralization. For example, HN—C═O, C—NH^{3+}, organic sulfides(S—C), cellulose, aldehydes, ketones, acetals, and organic acids, with inorganic salts may be related to the formation of crystals of the composite material to increase the hardness and stickiness[20]. These crystals on the shell plates are inorganic with organic molecules to control the formation of nanostructured condensed matter[21]. The shell is a successful case of the synthesis of multifunctional compound material in nature, and its peculiar structural character is one of the main reasons that result in its superior physical properties[22]. The composition of organic matter is multiple, and different layers differ greatly[3,23-25]. In the formation of the shell, biological macromolecule controls the development of crystals and, simultaneously, controls the shape of nanometer structure by adsorbing special single crystal face, increasing the hardness of material[20]. The nucleation, development, phases conversion and space location, of $CaCO_3$ crystal are all controlled strictly by biological macromolecules[3,20,26]. The study of organic matrix of shells is the key point to understand the mechanism of shell mineralization. It stressed the importance of $CaCO_3$ as the main component of shells and ignored the role of other inorganic salts in the past research data. NaCl and silicate were detected in all layers of the shell plate of *L. japonica*, magnesium sulfate was detected in many layers of the shell plate. Oxides such as Al_2O_3 and MgO were also detected in the shell plate. These substances play a direct role in the formation of the shell structure. Multi-layer structure, multi-order ultrastructure of the shell plate, and the pores on layer B, give the shell plates both characteristics of light weight and hardness. Structural characteristics are valuable for bionics and material science workers to refer to.

Acknowledgement:

The authors thank Prof. Xu Dongsheng (Low-dimensional Functional Nanomaterials Group, State Key Laboratory for Structural Chemistry of Unstable and Stable Species, Peking University) for providing the instruments and equipment, and for his various help. We also thank, Prof. Xie Jinglin (Testing and Analysis Center of Peking University) for giving some instructive advice on XPS analysis. We also thank Dr. Xu Lifen (Low-dimensional Functional Nanomaterials Group, Peking University) for giving some help during the observation of the ESEM specimens.

References

[1] Mao Zhenwei, Zhou Guien, Li Fanqing, *et al*. Study on microstructure of shell [J]. *Journal of Chinese Electron Microscopy Society*. 1996, **5**(6): 541 (Ch).

[2] Cuif J P, Dauphin Y. Occurrence of mineralization disturbances in nacreouslayers of cultivated pearls produced by *Pinctada margaritifera* var. *cumingi* from French Polynesia. Comparison with reported shell alterations [J]. *Aquatic Living Resources*, 1996, **9**: 187-193.

[3] Dauphin Y, Guzman N, Denis A, *et al*. Microstructure, nanostructure and composition of the shell of *Concholepas* (Gastropoda, Muricidae) [J]. *Aquatic Living Resource*, 2003, **16**(2): 95-103.

[4] Qi Zhongyan. *Economic Mollusca of China*[M]. Beijing: Agriculture Press of China, 1998: 25-26 (Ch).

[5] Qi Zhongyan, Ma Xiutong, Wang Zhenrei, *et al*. *Mollusca of Yellow Sea and Bohai Sea*[M]. Beijing: Agriculture Press of China, 1989: 4-13 (Ch).

[6] Chen Bin, Dong Qinjun, Wu Xiaojin, *et al*. Laminated microstructure of clam shell and research of biomimetic ceramic/polymer composite[J]. *Journal of Functional Materials*, 2004, **35**: 2345-2350 (Ch).

[7] Chen Junhao, Chen Guiqin. *The Crystal Structure of Shell*[M]. Qingdao: Qingdao Ocean University Press, 1993: 57-61 (Ch).

[8] Chen Junhao, Chen Guiqin. The crystal structure of pearl and its related shell[J]. *Acta Oceanologica Sinica*, 1987, **9**(6): 753-759 (Ch).

[9] Dauphin Y. The organic matrix of coleoid cephalopod shells: molecular weights and isoelectric properties of the matrix in relation to biomineralization processes [J]. *Marine Biology*, 1996, **125**(4): 525-529.

[10] Xie Zhongdong, Ding Xiaofei, Li Fengmin, *et al*. The structure characteristics of the shell of the conch *Hemifusus tuba*[J]. *Fisheries Science*, 2006, **25**(5): 253-255.

[11] Chateigner D, Hedegaard C, Wenk H R. Mollusc shell microstructures and crystallographic textures [J]. *Journal of Structural Geology*, 2000, **22**: 1723-1735.

[12] Laghi G F, Russo F. Shell structure and architecture of valves of *Chiton olivaceus* Spengler (Polyplacophora, Mollusca) [J]. *Bollettino della Società Paleontologica Italiana*, 1978, **17**(2): 272-291.

[13] Lei Xiaochun, Lu Lin, Li Kecheng. Fiber surface analysis with XPS, AFM, Tof-SIMS: Principle and Application [J]. *Transactions of China Pulp and Paper*, 2006, **21**(4): 97-101 (Ch).

[14] Aksay I A, Bae E, Sarikaya M, *et al*. *Hierarchically Structured Materials*[C]//*Proceedings of Materials Research Society*. Pittsburgh: Materials Research Society, 1992.

[15] Sarkaya M, Aksay I A. *Biomimetics*: *Design and Processing of Materials*[M]. New York: American Institute of Physics, 1996.

[16] Rodriguez-Navarro A B, CabraldeMelo C, Batista N, *et al*. Microstructure and crystallographic-texture of giant barnacle (*Austromegabalanus psittacus*) shell [J]. *Journal of Structural Biology*, 2006, **156**: 355-362.

[17] Li Fengmin, Zhao Jie, Wang Lai. Analysis for the structure characteristics and crystal orientation of shell of the conch *Hemifusus tuba* [J]. *Journal of Functional Materials*, 2004, **35**: 2342-2344 (Ch).

[18] Dauphin Y. Denis A. Structure and composition of the aragonitic crossed lamellar layers in six species of Bivalvia and Gastropoda [J].*Comparative Biochemistry and Physiology*, (Part A), 2000, **126**: 367-377.

[19] Neves N M, Mano J F. Structure/mechanical behavior relationships in crossed-lamellar sea shells [J]. *Materials Science and Engineering C*, 2005, **25**: 113-118.

[20] Belcher A M, Wu X H, Christensen R J, *et al*. Control of crystal phase switching and orientation by soluble mollusk-shell proteins [J]. *Nature*, 1996, **381**: 56-58.

[21] Berman A, Hanson J, Leiserowitz L, *et al.* Biological control of crystal texture: A widespread strategy for adapting crystal properties to function [J]. *Science*, 1993, **259**: 776-779.

[22] Heuer A H, Fink D J, Laraia V J. Innovative materials processing strategies: A biomimetic approach [J]. *Scienc*e, 1992, **255**: 1098-1099.

[23] Weiner S, Addadi L. Acidic macromolecules of mineralized tissues: the controllers of crystal formation [J]. *Trends in Biochemical Science*, 1991, **16**: 252-256.

[24] Falini G, Albeck S, Weiner S, *et al*. Control of aragonite or calcite polymorphism by mollusc shell macromolecules [J]. *Science*, 1996, **271**: 67-69.

[25] Cariolou M A, Morse D E. Purification and characterization of calcium-binding conchiolin shell peptides from the mollusk, *Haliotis rufescens*, as a function of development [J]. *Journal of Comparative Physiology*, 1988, **157B**(6): 717-729.

[26] Dauphin Y, Cuif J P, Doucet J, *et al*. *In situ* mapping of growth lines in the calcitic prismatic layer of mollusk shell using X-ray absorption near-edge structure (XANES) spectroscopy at the sulphur K-edge [J]. *Marine Biotechnology*, 2003, **142**: 299-304.

□